

Joint CMB and Weak Lensing Analysis; Physically Motivated Constraints on Cosmological Parameters

Carlo R. Contaldi,* Henk Hoekstra,† and Antony Lewis

CITA, University of Toronto, 60 St. George Street, Toronto, M5S 3H8, ON, Canada

(Dated: November 3, 2018)

We use Cosmic Microwave Background (CMB) observations together with the Red-sequence Cluster Survey (RCS) weak lensing results to derive constraints on a range of cosmological parameters. This particular choice of observations is motivated by their robust physical interpretation and complementarity. Our combined analysis, including a weak nucleosynthesis constraint, yields accurate determinations of a number of parameters including the amplitude of fluctuations $\sigma_8 = 0.89 \pm 0.05$ and matter density $\Omega_m = 0.30 \pm 0.03$. We also find a value for the Hubble parameter of $H_0 = 70 \pm 3 \text{ km s}^{-1} \text{ Mpc}^{-1}$, in good agreement with the Hubble Space Telescope (HST) key-project result. We conclude that the combination of CMB and weak lensing data provides some of the most powerful constraints available in cosmology today.

Keywords: Cosmology: Cosmic Microwave Background, Weak Lensing, Large Scale Structure, Dark Matter

The physics behind the anisotropies we see in the microwave background is well studied and understood [1]. The evolution of the photon distribution function in the tight coupling era and through decoupling is well inside the linear perturbation regime and is the reason for the CMB's unique status as a probe of cosmological models. The *physical* interpretation of the angular power spectrum of primary CMB anisotropies is unambiguous when restricted to the inflationary paradigm and given a suitably parametrized spectrum of initial perturbations.

The recently released WMAP first year results [2] have revealed the CMB angular power spectrum with unprecedented accuracy to multipoles below $\ell = 900$ [3]. The results are a stunning confirmation of the acoustic oscillation picture, with perturbations arising from an initial super-horizon spectrum of predominantly adiabatic fluctuations, as predicted for example by simple inflationary models. The measurements of the first two acoustic peaks has confirmed in precise detail earlier detections of the peak/dip pattern on scales below the sound horizon at last scattering [5, 6, 7, 8, 9, 10, 11].

On its own, the current picture of the CMB made up of the WMAP results together with high resolution CBI and ACBAR¹ observations implies tight constraints on a number of parameters [12, 13]; the curvature in units of critical density Ω_K and various other parameters in the combinations determined by the physical mechanisms which give rise to the observed CMB anisotropy. In addition the measurement of a cross-correlation between the polarization and temperature anisotropy [14, 15] is the first significant detection of reionization in the CMB, which gives a constraint on the optical depth to the last

scattering surface.

Although the CMB data alone provide tight constraints on some parameter combinations, other combinations are very poorly constrained due to partial degeneracies. The addition of other data such as measurements of the matter power spectrum $P(k)$ is essential to break these degeneracies and tightly constrain the parameters of most interest individually. One way to infer the matter power spectrum is to rely on visible tracers of the (dark) matter distribution such as galaxy redshift surveys or observations of the Lyman- α forest. The Lyman- α forest gives a way to measure the linear power spectrum of neutral gas at redshifts higher than those probed by galaxy surveys.

The combination of CMB, 2dFGRS [16], and Lyman- α forest data [18] yields tight constraints on the density of dark matter and vacuum energy, and also reveal an indication of a running of the scalar spectral index characterized by the parameter $dn_s/d \ln k$ [12]. However inferring the matter power spectrum using these techniques involves a heuristic treatment of the relation between the tracers and the dark matter usually referred to as 'biasing' [17]. As we enter the much heralded era of precision observations, such heuristic treatments might limit the accuracy with which parameters can be determined. A direct measurement of the power spectrum would not suffer from such limitations.

In terms of physical interpretation, measurements of the lensing signal induced by the LSS (cosmic shear) hold a unique position in the growing set of observational tools available to cosmologists; it is a *direct* probe of the projected matter power spectrum over a redshift range determined by the lensed sources and over scales ranging from the linear to non-linear regime. The intervening LSS induces a small, coherent correlation in the shapes of the background galaxies which nowadays can be measured accurately [19, 20, 21, 22, 23]. The use of weak lensing data is not without challenges: the small signal requires

*Electronic address: contaldi@cita.utoronto.ca

†Department of Astronomy & Astrophysics, University of Toronto, 60 St. George Street, Toronto, M5S 3H8, ON, Canada

¹ WMAPext combination

large survey areas and a careful removal of the observational distortions. However separation of the shear signal into gradient (“E-Type”) and curl (“B-Type”) components provides a control on systematics including the presence of intrinsic alignments of nearby galaxies or systematically induced distortions in the image. The RCS 53 sq. deg. results used in this work [24] have a low B-Type component on large scales together with a well determined redshift distribution of background sources.

In this *letter* we present results from cosmological parameter fits using only CMB and weak lensing data. The motivation for this approach is to provide constraints on parameters using only observables with robust physical interpretations.

To evaluate the posterior distribution of the parameters of interest from the data we use an extension of the publicly available Markov Chain Monte Carlo package COSMOMC², as described in [25]. We calculate the likelihood of each cosmological model with respect to a combination of CMB and RCS data. The CMB data consists of WMAP data below $\ell = 900$ and CBI, ACBAR, and VSA band powers above $\ell = 800$ where the WMAP data is noise dominated and hence the band powers are essentially independent. To compare each angular power spectrum to the WMAP data we use the likelihood calculation routine made available by the WMAP team³ [13].

For each model we also calculate the mass aperture variance $\langle M_{ap}^2(\theta) \rangle$ [26] at each aperture θ sampled by the RCS results [24]. The mass aperture variance is a narrow filter of the convergence power spectrum $P_\kappa(\ell)$ defined as

$$P_\kappa(\ell) = \frac{9}{4} \left(\frac{H_0}{c} \right)^4 \Omega_m^2 \int_0^{\chi_H} d\chi \frac{g^2(\chi)}{a^2(\chi)} P_{3D} \left(\frac{\ell}{f_K(\chi)}; \chi \right), \quad (1)$$

where χ is the radial coordinate and $f_K(\chi)$ is the comoving angular diameter distance to χ . $P_{3D}(k, \chi(z))$ is the 3D power spectrum of matter fluctuations. For each model we use the matter power spectrum calculated by CAMB [29] at $z = 0$ and rescale to $z > 0$ using the solution for growth of linear perturbations. To include the non-linear contribution to the power spectrum at each redshift we use the HALOFIT procedure [27]. The procedure has been calibrated using numerical simulations of structure formation and is significantly more accurate than the previous procedure by Peacock & Dodds [28]. In particular it reproduces accurately, with *rms* errors of a few percent, the full non-linear spectrum in standard Λ CDM models down to scales $k \sim 10h\text{Mpc}^{-1}$. The accuracy of the HALOFIT procedure is adequate for current weak lensing data although future surveys will require more accurate estimates of the full, non-linear power spectrum. This

will most probably require the use of large numbers of numerical simulations to calibrate directly the non-linear evolution in the full parameter space.

The function $g(\chi) = \int_\chi^{\chi_H} d\chi' p(\chi') f_K(\chi' - \chi) / f_K(\chi')$ is the source-averaged distance ratio where $p(\chi(z))$ describes the redshift distribution of sources in the shear survey which is approximated by the function $p(z) \sim (z/z_s)^\alpha \exp[-(z/z_s)^\beta]$. The values $\alpha = 4.7$, $\beta = 1.7$, and $z_s = 0.302$ give the best fit to the observed redshift distribution. To allow for the uncertainty in the mean redshift of the distribution we marginalize over the range of values $z_s \in [0.274, 0.337]$ for each likelihood evaluation. This corresponds to the $\pm 3\sigma$ range indicated by the χ^2 of the fit to the photometric redshift distribution. The mean redshift for this choice of parameters is $\langle z \rangle = 0.54 - 0.66$. We assume a Gaussian prior for z_s in this range.

For each model sampled by the Monte Carlo chain we calculate the log likelihood with respect to the RCS data

$$\ln L = -\frac{1}{2} \left(\langle \widetilde{M}_{ap}^2 \rangle_i - \langle M_{ap}^2 \rangle_i \right) C_{ij}^{-1} \left(\langle \widetilde{M}_{ap}^2 \rangle_j - \langle M_{ap}^2 \rangle_j \right), \quad (2)$$

where $\langle \widetilde{M}_{ap}^2 \rangle_i$ is the observed mass aperture variance at an aperture θ_i and C_{ij} is the covariance matrix of the data [24]. This result is added to the log likelihoods from the CMB fit for the same model to obtain the full likelihood with respect to both CMB and RCS data.

We sample the probabilities with respect to six basic cosmological parameters: the physical densities of baryons $\Omega_b h^2$, and cold dark matter $\Omega_c h^2$, the Hubble parameter $H_0 \equiv 100h \text{ km s}^{-1} \text{ Mpc}^{-1}$, a reionization redshift parameter z_{re} , and a constant spectral index n_s and amplitude A_s of the initial scalar curvature perturbations. We assume the universe is spatially flat, with purely adiabatic perturbations evolving according to General Relativity. The density of a cosmological constant type component Ω_Λ follows from $\Omega_\Lambda = 1.0 - \Omega_m$. We generated sixteen converged Monte Carlo chains using the CMB data only, removed burn in and thinned to obtain fairly independent samples. The matter power spectrum and RCS likelihood was then computed for each sample, and importance sampling used to adjust the chain weights accordingly (see [25]). The resultant set of weighted samples for the full posterior distribution from the CMB and RCS data were then used to compute our results. The only external prior assumed is a conservative big bang nucleosynthesis (BBN) Gaussian prior of the form $\Omega_b h^2 = 0.022 \pm 0.002 (1\sigma)$ [30]. We include this prior to partially break the remaining $n_s - \Omega_b h^2 - \tau - A_s$ degeneracy in the CMB data. The action of this is similar to the $\tau < 0.3$ prior adopted in the WMAP analysis [12, 13].

From the set of samples it is simple to also compute the posterior distribution of other derivable quantities such as the *rms* amplitude of matter fluctuations on $8h^{-1} \text{ Mpc}$ scales assuming linear evolution, σ_8 , the total matter den-

² <http://cosmologist.info/cosmomc/>

³ <http://lambda.gsfc.nasa.gov/>

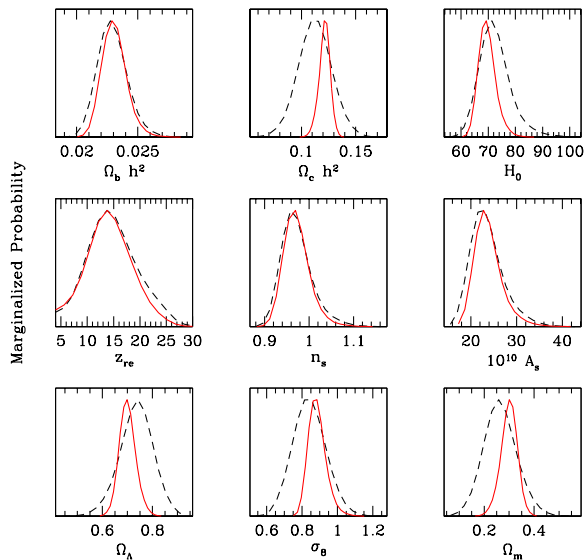


FIG. 1: One dimensional, marginalized probability distributions for a selection of parameters. The dashed (black) curves are for CMB only. The solid (red) curves include the RCS data. We see the weak lensing data, while being consistent with the CMB only results, narrow down a number of distributions considerably. In particular the combination of data provides a tight independent constraint on H_0 . The matter density and fluctuation amplitude are also much better constrained with the combination of CMB and weak lensing than with just CMB.

sity, Ω_m , the optical depth to last scattering, τ , and the age of the universe. In this letter we do not consider tensor perturbations, dynamical dark energy candidates, or a running spectral index. We will explore the constraints on these generalized models from CMB and weak lensing data future work.

The set of samples from the full six dimensional parameter space can be used to evaluate marginalized parameter distributions by evaluating the weighted number density of samples ignoring the values of the parameters marginalized over. In Fig. 1 we show the one dimensional marginalized distributions for a number of parameters. Each panel compares the distribution obtained using CMB data with that obtained using CMB and RCS data together; both also include the weak BBN prior discussed above. The effect of adding the weak lensing results is clearly seen in a number of parameters.

In Table I we summarize the marginalized constraints for a number of fundamental and derived parameters. We show the results obtained with and without inclusion of the RCS data. The addition of RCS data reduces the errors on σ_8 , Ω_m , H_0 , Ω_Λ , and $\Omega_c h^2$. We also show constraints on the ‘classical’ combinations probed by LSS data, namely, the constrained direction $\sigma_8 \Omega_m^{0.5}$ and the shape parameter $\Gamma \approx \Omega_m h$.

TABLE I: Marginalized constraints for a selection of parameters. The left column uses only CMB data, the right column is for CMB and RCS data. The only external prior included for both results is a Gaussian BBN prior of 0.022 ± 0.002 . All errors are 68% confidence intervals.

$(\Omega_{tot} = 1)$	BBN+CMB ^a	BBN+CMB ^a +RCS
$\Omega_b h^2$	0.023 ± 0.001	0.023 ± 0.001
$\Omega_c h^2$	0.112 ± 0.016	0.121 ± 0.005
h	0.73 ± 0.06	0.70 ± 0.03
z_{re}	15 ± 5	15 ± 4
n_s	0.97 ± 0.03	0.97 ± 0.03
$10^{10} A_s$	24 ± 4	25 ± 3
Ω_Λ	0.74 ± 0.07	0.70 ± 0.03
Ω_m	0.26 ± 0.07	0.30 ± 0.03
T_0 (Gyrs)	13.6 ± 0.3	13.6 ± 0.2
σ_8	0.84 ± 0.09	0.89 ± 0.05
$\sigma_8 e^{-\tau}$	0.73 ± 0.08	0.78 ± 0.02
$\sigma_8 \Omega_m^{0.5}$	0.43 ± 0.09	0.48 ± 0.02
$\Omega_m h$	0.19 ± 0.03	0.21 ± 0.01
$\Omega_m h^{2.3} (\sigma_8 e^{-\tau})^{-0.9}$	0.163 ± 0.003	0.162 ± 0.002

^aWMAP($\ell < 900$) + CBI,ACBAR,VSA($\ell > 800$)

It is instructive to look at the marginalized, two dimensional likelihood in the (Ω_m, σ_8) plane to understand how drastic improvements in the determination of the two parameters are obtained (Fig. 2). The RCS data alone is near degenerate in a particular direction while CMB data alone provides broad constraints in a *quasi*-orthogonal direction to RCS. The combination of the two data sets give a much tighter confidence region. The region of intersection in six dimensions has slightly above average CMB likelihood, as is readily assessed using the importance weighted samples, so the data sets are highly consistent even in the full parameter space. The spread of the CMB posterior in the direction of the RCS degeneracy is largely due to the uncertainty remaining in the optical depth, as is clear for the tight constraint for $\sigma_8 e^{-\tau}$ given in Table I.

Overall our results are consistent with similar constraints from a combination of CMB, 2dFGRS, and Lyman- α data [2, 12] with similar or smaller errors. The values obtained for σ_8 using the WMAP data are somewhat higher than those obtained previously from CMB data due to the new evidence for a significant optical depth and a slightly higher anisotropy amplitude than previous observations indicated [3]. This is still lower, although not inconsistent, with estimates of σ_8 from a possible Sunyaev-Zeldovich Effect (SZE) contribution to the CMB power spectrum at high- ℓ . The latest estimates using the CBI deep-field results [31, 32] and ACBAR and BIMA [33] data suggests a value of $\sigma_8^{SZ} = 0.98_{-0.21}^{+0.12}$ [34] with large errors due mainly to the non-Gaussian nature of the SZE. Increasingly accurate measurements of the CMB power spectrum at high- ℓ will reduce these errors drastically and comparing the two independent determi-

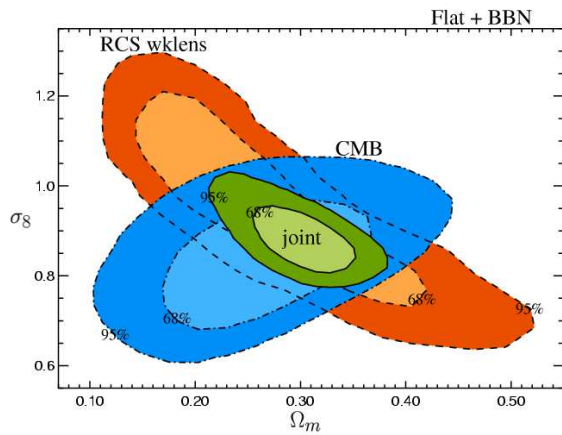


FIG. 2: The two dimensional, marginalized likelihoods for the (Ω_m, σ_8) plane. The overlaid, filled contours show the 68% and 95% integration levels for the distributions. Bottom – RCS only, Middle – CMB only, Top – CMB+RCS.

nations of σ_8 will be useful in increasing our understanding of the cluster properties that determine the SZE.

Our result for the Hubble parameter is consistent within 1σ with the HST key-project result [35] but has smaller errors. Similarly, the value for the matter density $\Omega_m = 0.30 \pm 0.03$ is consistent with other determinations. The addition of RCS data leave estimates of the scalar spectral tilt n_s essentially unaffected. This is due to the small range of scales probed by the RCS weak lensing results. Future surveys will most certainly have much more leverage on n_s as they will probe a range in scales an order of magnitude larger.

We have shown how CMB and weak lensing results can be combined to obtain constraints on cosmological parameters that depend on observations that have simple physical interpretations. Although only first generation weak lensing data are currently available our approach yields results with errors comparable to or even smaller than those obtained using CMB in combination with other types of surveys. These results are encouraging for the use of next generation weak lensing surveys in deriving robust parameter fits. In particular the Canada–France–Hawaii–Telescope (CFHT) Legacy Survey ~ 170 sq. deg. cosmic shear project will be a major step forward in the field of weak lensing.

The increasing accuracy in the determination of the source redshift distribution in future surveys will also help in reducing uncertainties and systematics tied to any intrinsic alignment in the ellipticity of nearby sources. It will also introduce the possibility of resolving separate redshift contributions to the convergence power spectrum (Eq. 1) thus enhancing the parameter fitting ability of the observations.

We conclude that the combined CMB, weak lensing approach to parameter determination already constitutes a competitive alternative to other combinations and holds

much promise for future investigations.

It is a pleasure to thank Dick Bond, Ue-Li Pen, and Dmitry Pogosyan for useful discussions. We acknowledge the RCS team for use of their data. Research at CITA is supported by NSERC and the Canadian Institute for Advanced Research. The computational facilities at CITA are funded by the Canadian Fund for Innovation. CRC acknowledges the Kavli Institute for Theoretical Physics (National Science Foundation Grant No. PHY99-07949) where part of this work was carried out.

-
- [1] J. R. Bond, in “Cosmology and large scale structure”, Les Houches Session LX, eds., R. Shaeffer, J. Silk, M. Spiro, and J. Zinn-Justin (Elsevier), pp. 469-674
 - [2] C. L. Bennett *et al.*, [arXiv:astro-ph/0302207].
 - [3] G. Hinshaw *et al.*, [arXiv:astro-ph/0302217].
 - [4] D. H. Lyth and A. Riotto, Phys. Rept. **314**, 1 (1999).
 - [5] Miller, A.D. *et al.*, Astrophys. J. , **524**, L1, (1999).
 - [6] J. E. Ruhl *et al.*, [arXiv:astro-ph/0212229].
 - [7] Lee, A. T. *et al.*, Astrophys. J. , **561**, L1, (2001).
 - [8] Halverson, N. W. *et al.*, Astrophys. J. , **568**, 38 (2002).
 - [9] T. J. Pearson *et al.*, [arXiv:astro-ph/0205388].
 - [10] K. Grainge *et al.*, [arXiv:astro-ph/0212495].
 - [11] C. I. Kuo *et al.*, [arXiv:astro-ph/0212289].
 - [12] D. N. Spergel *et al.*, [arXiv:astro-ph/0302209].
 - [13] L. Verde *et al.*, [arXiv:astro-ph/0302218].
 - [14] A. Kogut *et al.*, [arXiv:astro-ph/0302213].
 - [15] L. Page *et al.*, [arXiv:astro-ph/0302220].
 - [16] M. Colless *et al.*, MNRAS, **328**, 1039, (2001).
 - [17] N. Kaiser, Astrophys. J. **284**, L9, (1984).
 - [18] Croft, R.A.C. *et al.*, Astrophys. J. , **581**, 20, (2002).
 - [19] D. Bacon, A. Refregier and R. Ellis, MNRAS, **318**, 625, (2000).
 - [20] H. Hoekstra, H. K. Yee, M. D. Gladders, L. F. Barrientos, P. B. Hall and L. Infante, [arXiv:astro-ph/0202285].
 - [21] N. Kaiser, G. Wilson and G. A. Luppino, [arXiv:astro-ph/0003338].
 - [22] L. van Waerbeke *et al.*, A&A, **358**, 30 (2000).
 - [23] L. van Waerbeke, Y. Mellier, R. Pello, U. L. Pen, H. J. McCracken and B. Jain, Astron. Astrophys. **393**, 369 (2002).
 - [24] H. Hoekstra, H. Yee and M. Gladders, Astrophys. J. **577**, 595 (2002).
 - [25] A. Lewis and S. Bridle, Phys. Rev. D **66**, 103511 (2002).
 - [26] P. Schneider, L. van Waerbeke, B. Jain and G. Kruse, MNRAS, **296**, 873, (1998).
 - [27] R. E. Smith *et al.*, [arXiv:astro-ph/0207664].
 - [28] J. A. Peacock and S. J. Dodds, MNRAS, **280**, L19, (1996).
 - [29] A. Lewis, A. Challinor and A. Lasenby, Astrophys. J. **538**, 473 (2000).
 - [30] D. Tytler, J. M. O’Meara, N. Suzuki and D. Lubin, [arXiv:astro-ph/0001318].
 - [31] J. R. Bond *et al.*, [arXiv:astro-ph/0205386].
 - [32] B. S. Mason *et al.*, [arXiv:astro-ph/0205384].
 - [33] K. S. Dawson *et al.*, Astrophys. J. **581**, 86 (2002)
 - [34] J. H. Goldstein *et al.*, [arXiv:astro-ph/0212517].
 - [35] W. L. Freedman *et al.*, Astrophys. J. **553**, 47 (2001).